LBL-24519
UC-21

Lawrence Berkeley Laboratory
UNIVERSITY OF CALIFORNIA

Accelerator & Fusion Research Division

RECEIVED
LAWRENCE
BERKELEY LABORATORY

FEB 19 1988

LIBRARY AND
DOCUMENTS SECTION

Heavy Ion Fusion Accelerator Research (HIFAR)
Year-End Report: April 1, 1987–September 30, 1987

Heavy Ion Fusion Staff

December 1987

TWO-WEEK LOAN COPY
This is a Library Circulating Copy which may be borrowed for two weeks.

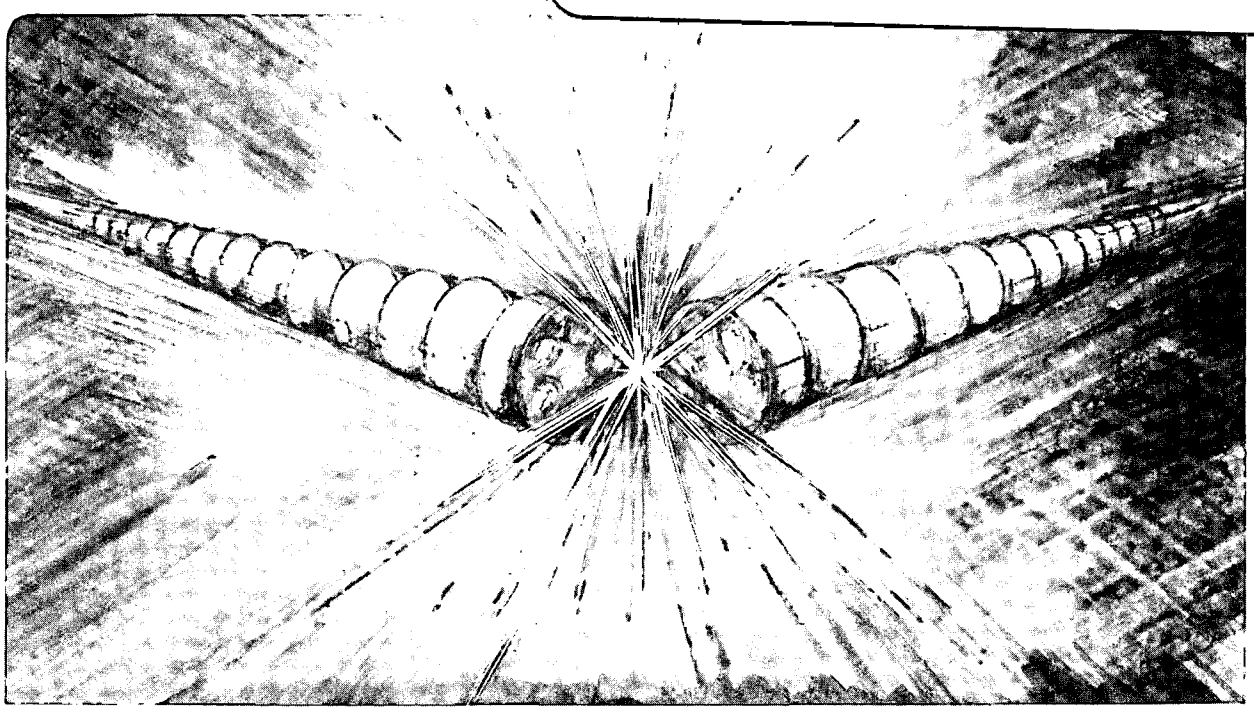

Prepared for the U.S. Department of Energy under Contract DE-AC03-76SF00098

LBL-24519 c.2

DISCLAIMER

This document was prepared as an account of work sponsored by the United States Government. While this document is believed to contain correct information, neither the United States Government nor any agency thereof, nor the Regents of the University of California, nor any of their employees, makes any warranty, express or implied, or assumes any legal responsibility for the accuracy, completeness, or usefulness of any information, apparatus, product, or process disclosed, or represents that its use would not infringe privately owned rights. Reference herein to any specific commercial product, process, or service by its trade name, trademark, manufacturer, or otherwise, does not necessarily constitute or imply its endorsement, recommendation, or favoring by the United States Government or any agency thereof, or the Regents of the University of California. The views and opinions of authors expressed herein do not necessarily state or reflect those of the United States Government or any agency thereof or the Regents of the University of California.

LBL-24519
HIFAN-380

HEAVY ION FUSION ACCELERATOR RESEARCH (HIFAR)

YEAR-END REPORT*

April 1, 1987 - September 30, 1987

Heavy Ion Fusion Staff

Accelerator and Fusion Resarch

Lawrence Berkeley Laboratory
University of California
Berkeley, CA 94720

December 1987

Attention: This document is provided for DOE "Official Use". Distribution to other interested parties is made with the understanding that no information or experimental results given herein will be quoted without first obtaining the authors' permission, or until such information or results have appeared in the open literature.

*This work was supported by the Office of Energy Research, Office of Basic Energy Sciences, U.S. Department of Energy under Contract No. DE-AC03-76SF00098.

FOREWORD

The basic objective of the Heavy Ion Fusion Accelerator Research (HIFAR) program is to assess the suitability of heavy ion accelerators as igniters for Inertial Confinement Fusion (ICF). A specific accelerator technology, the induction linac, has been studied at the Lawrence Berkeley Laboratory and has reached the point at which its viability for ICF applications can be assessed over the next few years.

The HIFAR program addresses the generation of high-power, high-brightness beams of heavy ions, the understanding of the scaling laws in this novel physics regime, and the validation of new accelerator strategies, to cut costs. Key elements to be addressed include: 1) Beam quality limits set by transverse and longitudinal beam physics; 2) Development of induction accelerating modules, and multiple-beam hardware, at affordable costs; 3) Acceleration of multiple beams with current amplification -- both new features in a linac -- without significant dilution of the optical quality of the beams; 4) Final bunching, transport, and accurate focussing on a small target.

TABLE OF CONTENTS

	Page
Highlights	1
MBE-4 Mechanical Progress	3
Alignment of MBE-4	4
A Compact Energy Analyzer for MBE-4	5
Cs^+ Injector Modeling with the Egun Code	6
An Improved Emittance Scanning System for HIFAR	7
2-MV Injector	8
Carbon Arc Source Development	9
Beam Combining in ILSE.	10
Emittance Growth Due to Transverse Beam Combining in ILSE -- Analytical Results	11
Transverse Beam Combining in ILSE -- Particle Simulation Results	12
Achromatic Beam Combiner for ILSE	13
Additional Elements for Beam Merging	14
Quadrupole Magnet Design for ILSE	15
Waveforms and Longitudinal Beam-Parameters for ILSE	16
Publications and Internal Notes	17

HIF Staff Roster 24

Distribution List 25

HIGHLIGHTS

D. Keefe

1. A major milestone reached in the past fiscal year was the installation of the final complement of components for the MBE-4 apparatus. Completion occurred within a few weeks of the projected date based on a schedule set two years ago. The accelerator was extensively surveyed and the focussing elements aligned to within ± 5 mils (rms) over the 17-meter length.

2. Current-amplification experiments were last made six months ago at the end of 12 accelerator units (reported in Half-Year Report of Mar. 31, 1987, LBL-23168). Further experiments of this kind have not been possible during the installation of the final 12 accelerating units. The opportunity was taken to improve the diagnostic capabilities; a compact energy analyzer was developed and installed in the upstream part of MBE-4 and more powerful software developed for reducing the emittance data. In addition, the emittance of the beam was studied at the exit of the injector and after the early lenses of the matching section; some emittance growth is observed as the beam passes the first two matching lenses, where the beam fills essentially the entire aperture.

3. The pressure vessel, graded column and other parts for the 2-MV injector arrived at LBL from LANL towards the end of this reporting period. Space was prepared in the basement of Building 58 and assembly begun.

4. The 200-kV injector for the Single-Beam Transport Experiment (SBTE) is being used as a test-stand for study of the UNM carbon arc source developed by Humphries. The gating system, which prevents plasma pre-fill of the diode and so allows rapid turn-on of the beam, works well. The maximum observed current density of 24.5 mA/cm^2 is very close

to the desired design value for ILSE (25 mA/cm^2). Modifications are being made to the trigger arc to improve lifetime and stability.

5. A self-consistent baseline physics design for the Induction Linac System Experiment (ILSE) is nearing completion. A major preoccupation of the group has been the understanding of the physics of the combining section at the 4-MeV point, and the conceptual design and layout of the electric/magnetic lenses and bending elements making up the combining section. Two candidate systems studied comprise a non-achromatic all-electrostatic system (reported in Mid-Year Report, Mar. 31, 1987, LBL-23168) which must be rapidly pulsed to accommodate the velocity tilt, and an achromatic system made of mixed electric and magnetic elements. There now exist designs for the close-packed quadrupoles for the four beams just upstream of the unification point and, also, for the quadrupoles in the linac section beyond the combining section. An asymmetric stacking of the four beams is harder to accommodate than a symmetric stacking, but is calculated to result in significantly less emittance growth in the final beam.

With the help of the SLID code, a reference design for the longitudinal acceleration schedule has been developed. The use of a light ion (carbon) and the constraints on physical length and on the momentum tilt make this a more difficult design problem than for a longer linac (longer in a scaled sense), such as MBE-4 or a driver.

MBE-4 MECHANICAL PROGRESS

D. Vanecek and R. Hipple

The last half of FY1987 saw completion of the major hardware for the Multiple-Beam Experiment, MBE-4, with the installation of Section "D" acceleration units, the installation of Section "E" transport and acceleration units, and the fabrication and installation of Section "F" transport and acceleration units. (See Fig. 1.) A typical acceleration core arrangement for Sections "D, E, or F" is shown diagrammatically in Fig. 2. The transport column design of Sections "D, E, and F" differ from Sections "A, B, and C" in two areas, 1) the acceleration gap is shortened from 5.9" to 0.5" by the installation of re-entrant tubes as shown diagrammatically in Fig. 2 and photographically in Fig. 3, and 2) these acceleration columns are rotated 90° from the previous Sections to allow the high voltage feedthroughs to enter vertically from above the transport columns. These high voltage feedthroughs are longer to accommodate the higher focusing voltages. This brings to a conclusion the fabrication and installation of the transport and acceleration portions of the MBE-4 apparatus. (See photograph of Fig. 4.)

The diagnostic portion of the MBE-4 Program will be an ongoing activity. At this writing we have a full complement of faraday cups and three sets of emittance slits and slit-cups, as well as other diagnostic hardware as shown diagrammatically in Fig. 6. We are in the process of fabricating more and better emittance slits and slit-cups as well as other specialized diagnostic hardware.

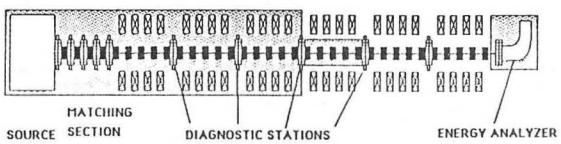

Fig. 1. The solid lines enclose the parts of MBE-4 apparatus in place in March, 1987. The other units and their associated electronics have now been added.

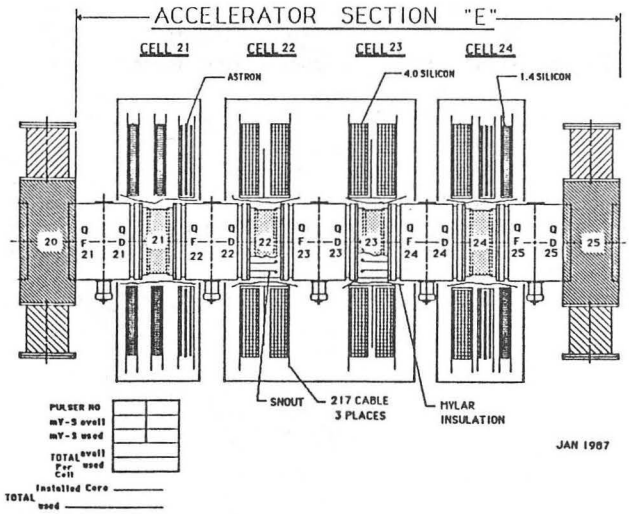

Fig. 2. The cores in both Cells 22 and 23 are driven from a single 120-kV spark-gap pulser. To minimize the transit-time between these cells (the better to utilize the core volt-seconds) tubular snouts were added as shown to decrease the inter-gap distance.

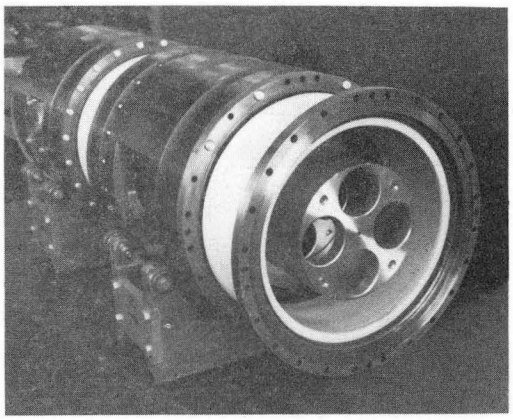

Fig. 3. Close-up of the shortened accelerating gap.

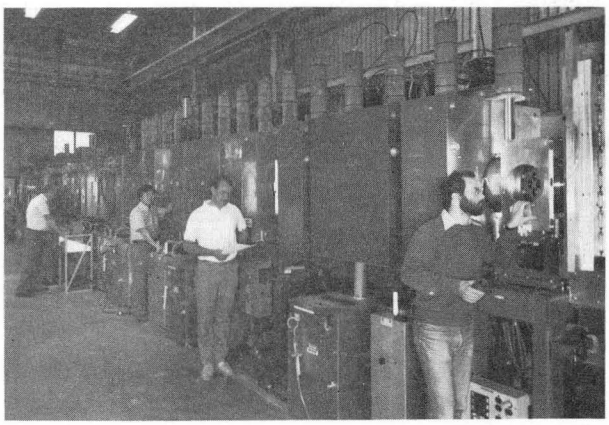

Fig. 4. H. Meuth, A. Warwick, C. Kim and T. Fessenden with the completed MBE-4 hardware.

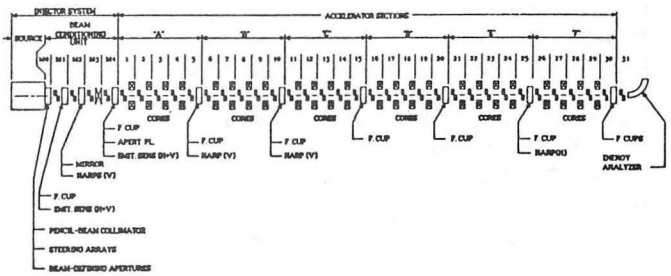

Fig. 5. Location of diagnostics.

ALIGNMENT OF MBE-4

H. Meuth, R. Hipple, W. Tiffany, and D. Vanecek

Summary

As a part of the completion of the MBE-4 apparatus, we carefully re-examined the alignment of MBE-4 including effects produced by vacuum loading. To date we have achieved an alignment of the reference axes of the "south" and "north" beams to within ± 0.005" rms with an absolute maximum error between two readings of 0.010", at ambient air pressure.

Vacuum Loading

Earlier this half-year period we examined the diode shear and distortion caused by vacuum loading. Large differential forces between the Marx tank and the source box introduce a lateral displacement of the centers of the four cesium sources with respect to the reference axis. The references axes are defined by the centers of the holes in the cathode plate at the injector exit and by the centers of the quadrupoles at box M25. The graphite anode that carries the thermionic emitters is mounted on a cantilevered, elbow-type feedthrough to the Marx tank, positioned at a right angle to the machine axis. The lateral travel of the anode plate at vacuum pump down was measured with feeler gauges to be about 0.050". An additional initial motion of approximately 0.030" was also observed, but thereafter the lateral travel was reproducible to within a few mils under repeated vacuum cycling. However, we expect that these measurements will not remain constant with time or with extended operation.

To ensure satisfactory alignment under experimental conditions, we will recheck these measurements prior to resuming the MBE-4 experiments. For this purpose we have drilled a ≈ .040" hole in the center of the four cesium sources. When the sources are hot the hole appears as a white dot that is easily seen in our alignment transits.

Alignment at Atmospheric Pressure

We report here the results of the MBE-4 alignment that was performed under ambient air pressure. The accelerator columns consisting of four lattice periods and accelerating gaps are assembled and pre-aligned on a bench setup (1). These are joined by the diagnostic boxes which have adjustments for alignment. During the assembly of MBE-4, alignment of the columns and boxes was performed with the aid of two Brunson Surveyer's transits set up parallel to the "south" and "north" beam axes. The angular position of the column was checked by inserting targets into either endplate. For each box, the vertical position and rotation about the horizontal transverse axis (F_H) were adjusted by four-point shimming. The horizontal position was adjusted by two set screws laterally threaded into the cradle supporting each box. Rotation around the vertical axis was adjusted by four set screws operating in the longitudinal direction. (See Fig. 1.)

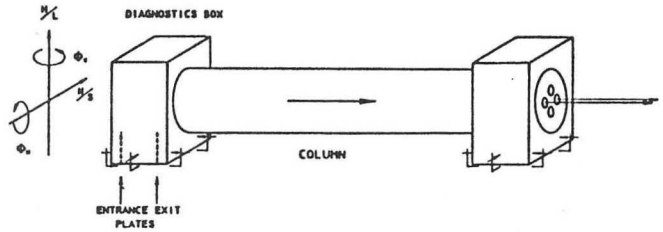

Fig. 1. Location of set-screws for adjustment.

Within the matching section, the individual quadrupole barrels cannot be aligned. However, by adjusting the matching-section bed as a whole we were able to achieve satisfactory alignment by minimizing the mean deviation from the two reference axes.

Results

Figure 2 shows the horizontal and vertical alignment along MBE-4 that was achieved by these procedures.

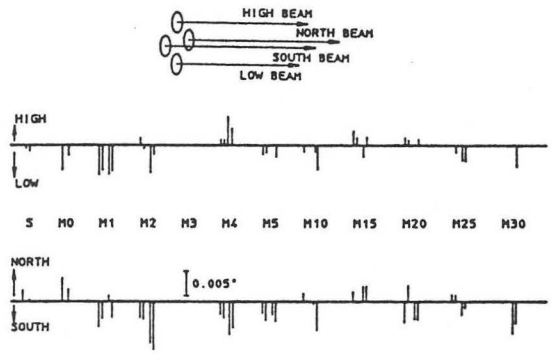

Fig. 2. Transverse displacements from reference axis.

References

1. T. Henderson and J. Meneghetti, "Four-Beam Electrostatic Quadrupole Doublet Assemblies", HIFAR Year-End Report: FY-85, LBL-20310, p. 9, October 1985.

A COMPACT ENERGY ANALYZER FOR MBE-4

H. Meuth and W.B. Ghiorso

Introduction and Summary

A small electrostatic energy analyzer (see Fig. 1) similar to that at the end of MBE-4 but only one-fifth the size was built. It is small enough that it can be inserted into any of the diagnostic boxes of MBE-4. Because of voltage breakdown limitations the analyzer can not be used at beam energies much above 300 keV. Therefore, it is useful for determining the beam energy at the entrance to the accelerator, after Section A, and possibly after Section B. With horizontal insertion, either of the horizontal MBE-4 beams can be monitored. Beam loading of the analyzer electrodes is negligible, and the effects of beam spill from the three adjacent beams is avoided by shielding. High-integrity electrical shielding was partially successful in rejecting the transient injector noise that arrives nearly simultaneously with the beam signal. First energy scans at the diagnostic boxes M1 and M4 compare well with scans taken with the large end-analyzer during the early stage of MBE-4 construction.

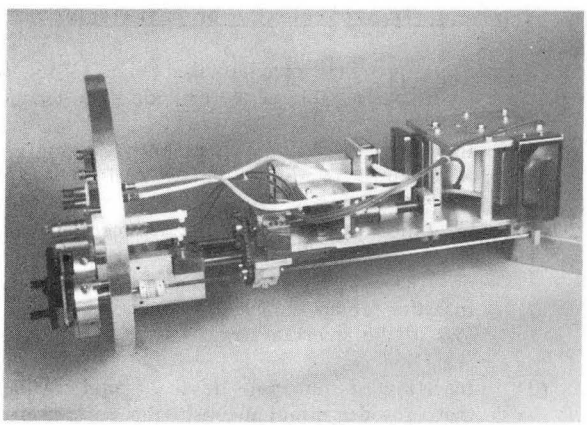

Fig. 1. Compact Energy Analyzer

Design Features

The original rationale and design for a small analyzer that could fit inside the diagnostic boxes and thus provide time-dependent beam energy information at the entrance to the accelerator were first examined by D. Keefe [1]. The analyzer consists of two coaxial cylindrical electrodes with a radial spacing of d = 1 cm and a mean radius of r = 10 cm. The electrodes extend over slightly less than a quadrant. Entrance and exit snouts, constrained by the focusing quadrupoles, are used to localize the analyzing field to the region of the electrodes. The radial deflecting field is effective over an arc of 90°. Both object and image slit widths are 0.010". We estimate (for the limit of zero space charge) the focal plane to be at a distance of 1.9" behind the (image) quadrant point. An estimate of the effects of space charge obtained by scaling the results for the large end-analyzer [2,3] yields a distance of 3 1/4" for the location of the focal plane. The position of the detector can be externally adjusted from 0.7" to 4.5". To allow for small errors in the alignment of the entrance slit and the detector, the detector can be rotated with respect to the axis of the electrodes. The electrodes will withstand at least 42 kV which is approximately the voltage needed to analyze singly-charged ions at 200 kV. We have not yet determined the absolute stand-off capability limit. It is conceivable that the actual limit will permits ion energy measurements after the first and possibly even after the second accelerator sections.

The analyzer can detect either of the two beams situated along its insertion direction. To date, the analyzer has been inserted horizontally to characterize the "left" and the "right" beams.

Measurements

Measurements were performed to examine the effects of beam loading and beam spill on the analyzer. These could momentarily alter the analyzing voltage resulting in an error in the energy determination. The maximum voltage excursion when operating the analyzer at 40 kV was 20V, which is negligible.

We determined the energy profile of the beam with time at box M1 and at box M4. These results were compared with measurements of the beam at M1 obtained with the large end-analyzer by Warwick [4] . Although good agreement was found, a discrepancy of approximately 5% in the absolute beam energy remained.

References

1. D. Keefe, "Energy Analysis for MBE-4", HIFAR Note-106, Nov. 12, 1986.

2. A. Faltens and S. Rosenblum, HIFAR Note-17.

3. A.H. Sato, HI-FAN-296.

4. A. Warwick, HIFAR Note-35; T.J. Fessenden et al., Conf. Proc. Heavy Ion Inertial Fusion 1986, p. 145.

Cs^+ INJECTOR MODELING WITH THE EGUN CODE

H. Meuth

Introduction and Summary

In the course of efforts to align the MBE-4 experiment, we have modeled the entire Cs^+ injector up to the first quadrupole of the matching section. We detected several potential aberrations:

(a) A shear due to lateral mis-alignment in the diode configuration leads to angular beam deflection.

(b) Slight tilting of the cesium sources produces little change in beam angle and, consequently, can not be used for beam steering. Conversely, small source mounting errors do not pose a sensitive alignment issue.

(c) Overfocussing of the outermost beam trajectories leads eventually to a paraxial beam component with large (negative) divergence angles.

(d) The MBE-4 beams enter the first quadrupoles with a maximum divergence angle of about 30 mrad.

Possible improvements in the MBE-4 source-to-matching-section interface suggested by these calculations are discussed.

Diode Shear and Emitter Tilting

Because of the nature of the EGUN code that models only azimuthally symmetric geometries, these two effects were examined with a "hollow" beam. A lateral off-axis displacement of the cathode plate (located at z = 136 mm) by 2 mm inwards led to a net beam displacement (at z = 200 mm) of about 1.5 mm outwards, and an angular beam deflection of 5 mrad. The cathode plane and the anode plane were kept parallel. This deflection is caused by the lens action of the cathode hole.

The tilting of the source cups and thereby the emitter surface equipotential plane with respect to the plane of the graphite anode plate and the cathode plane had no effect on beam angle, position and divergence. Tilts up to 20 mrad were examined. This result is to be expected on the basis of the anode-plate configuration that forms approximately spherical equipotential surface at the emitter plane, making it insensitive to small tilts of the emitter cups.

Overfocussing and Divergence of the Space-Charge Dominated Source

We have modeled the single beam configuration with anode, cathode and steerer array up to the plane of entrance into the first quadrupole. We determined the beam divergence vs. beam radius at the various axial positions of interest. At the cathode plate (z = 134 mm) the source aberrations have already led to the crossing of the outermost beamlets into the beam interior. While there is no provision for a beam-limiting aperture at this axial location, an aperture there of 15 mm diameter could essentially eliminate the aberrant outer rays, but would reduce the total current by about a factor of 2. The aperture plate is presently located at the entrance to the first quadrupole (z = 284 mm). The two aperture diameters available are labeled "5mA" and "10 mA." We note a maximum outer-ray divergence in excess of 30 mrad. This divergence can only be marginally reduced by the "10 mA" aperture. The "5mA" aperture reduces the maximum divergence to about 17 mrad, a value more in line with the focussing capability of the MBE-4 matching section.

Possible Improvements or Strategies

(a) A first aperture that restricts the beam to its non-aberrant part is desirable at the cathode plate location.

(b) The beam divergence halved for proper focussing in the matching section. Three options are available for this:

(1) Operation of MBE-4 at the reduced current of 5 mA per beamlet.

(2) Insertion of an einzel lens, at the expense and loss of the steering array.

(3) Insertion of multipole device ("squirrel cage") that provides simultaneously the crossed dipole fields for steering and the quadrupole fields for lateral beam confinement.

Note that options (2) to (3) involve substantial modifications to the MBE-4 source-to-matching section interface.

AN IMPROVED EMITTANCE SCANNING SYSTEM FOR HIFAR

S.H. McCreight

Important measurements in the experiments of the HIFAR program are of the transverse parameters of the beams as functions of length along the experments and of time in the pulse. In our experiments, measurements of these parameters are made using the "two-slit method". The principle of the measurements of the beamlet passing through the two slits we obtain: the mean position of the beam in the focusing channel; the rms beam size; the mean angle of the beam with respect to the axis; and a measure of the random transverse velocity of the beam. The beam size and transverse velocity are combined to determine the beam emittance.

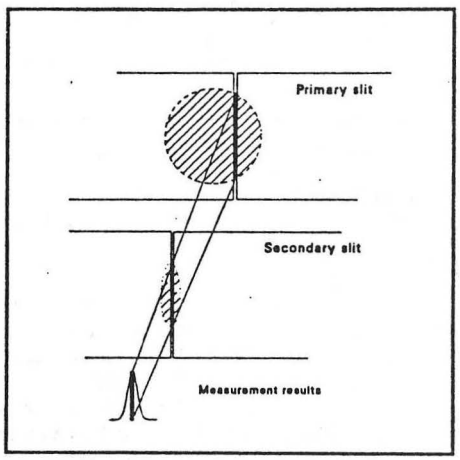

Fig. 1. Illustration of the principle of the two-slit phase-space measurement technique. The particles are collimated in position by the upstream slit, and the downstream slit passes those particles into the detector which have a certain well-defined transverse velocity.

The first system used to measure emittance was developed by W. Ghiorso and S. Rosenblum (1) and by M. Tiefenback (2). The positions of the two slits were adjusted by stepping motors that were controlled by a HP-85 computer. The beam current passing through the two slits was detected by a Faraday cup coupled to a sampling oscilloscope. The signal from a single sampling interval was passed to the computer which, given the position of the two slits, calculated the phase space parameters of the beam. A typical measurement at one point in space and a few nanoseconds in time required approximately 1000 shots of the machine or about 5000 seconds of real time. Thus obtaining emittance measurements as a function of time in the pulse at a given location required many hours of experimentation.

In 1987 a new computer-controlled system was developed that allows the transverse beam parameters and emittances of the MBE-4 and SBTE beams to be measured at up to 50 sampling intervals during every shot. This saves many hours of experimental time and allows all time information to be collected in one experiment. The stepper motors and sampling oscilloscope were interfaced to an IBM PC computer running a Pascal program. The added speed of the compiled program allows much more data to be taken during each shot of the machine. Several utilities were also developed, that allow the operator to set-up experiment in about 10 minutes, whereas the older system often required hours. Once the data have been taken, an analysis program called DISPLAY is used to plot the phase elippse and perform a number of other calculations. DISPLAY has the capacity to show up to four separate data files on the screen on once or four separate attributes of the same file. Some of the more important functions of DISPLAY are shown in Figs. 2 and 3.

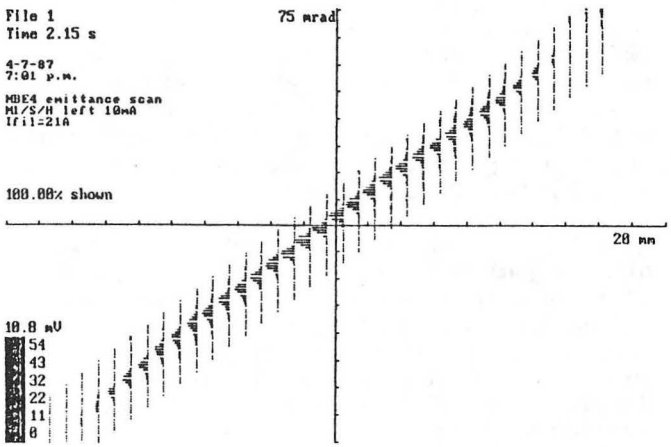

Fig. 2. Phase Ellipse at 2.15 μs

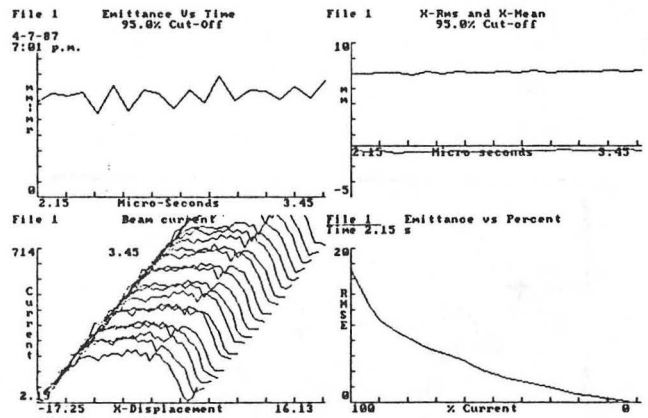

Fig. 3. Time-dependent characteristics of the beam

References

1. W.B. Ghiorso and S.S. Rosenblum, An Automated System for Envelope and Emittance Measurement, LBID-880 and HI-FAN-242, Lawrence Berkeley Laboratory, March 1984.

2. M.G. Tiefenback, Ph.D. Thesis, Space-Charge Limits on the Transport of Ion Beams in a Long Alternating Gradient System, LBL-22465, Lawrence Berkeley Laboratory, November 1986.

2-MV INJECTOR

H.L. Rutkowski

The last six months have been a period of transition for the 2-MV Injector. The Los Alamos group has terminated their involvement in the project and the parts have been shipped to LBL. During this period LBL personnel have made several trips to Los Alamos in order to expedite the transfer of effort.

There have been three main areas of progress on the injector. First, the ceramic insulators in which the accelerator column will reside, had fillets remaining from the braze process. These fillets would cause problems if high voltage were applied to the insulator. After discarding a variety of processes for safety reasons, a series of acid baths was chosen. The braze material was first electrostripped in a 1%HNO_3-1%KNO_3 bath. Then a titanium residue was removed in an HF-HNO_3 bath. These operations required considerable special handling because of the value and size of the insulator columns (100 k$ and 200 lbs each).

The second area is the pulsed power system. The triggering jitter in the Marx generator was approximately 125 ns when the 750 kV system was first assembled. After changing the trigger system by installing bypass capacitors across half the trigger resistors, the jitter was reduced to 10 ns. The capacitor mounting trays in the Marx were designed to be 6.25 inches apart. This design value was experimentaly verified as safe by placing the last three trays at this separation and charging to full voltage. This number is important to verify because the design has been changed from a conventional Marx to an inductively graded Marx using more trays. The reason for the change is to improve voltage grading along the accelerator column by using a 20-microsecond critically damped discharge. This new design will require eighteen trays instead of the original twelve, thus making the overall structure longer. Using the minimum safe tray spacing minimizes the required lengthening of the support beams and the lengthening of the pressure vessel. Lucite castings for the new inductive rings which replace the old corona rings are now available for machining. The additional capacitors, trays, and spark gaps will be delivered very shortly.

The third area is the mechanical design and fabrication of the system. A new prototype clamp ring for the electrodes was designed and tested successfully. A trial assembly of the insulator column with all its external hardware was made successfully in the pressure vessel. The motor-generator drive-shaft survived several full-load impulse tests with no signs of damage. Various detailed designs and conceptual designs were completed.

All of the above work with the exception of the Marx redesign was performed at LANL by E. Meyer and J. Umphres.

An area in building 58 has now been prepared to receive the injector and all of the parts have been shipped to LBL. Reassembly of the Los Alamos Marx configuration is underway and the additional parts for the 2-MV generator are being received soon. Once the 750 kV Marx is run successfully here, and the high voltage fabrication techniques are finalized, assembly of the full 2-MV generator will begin.

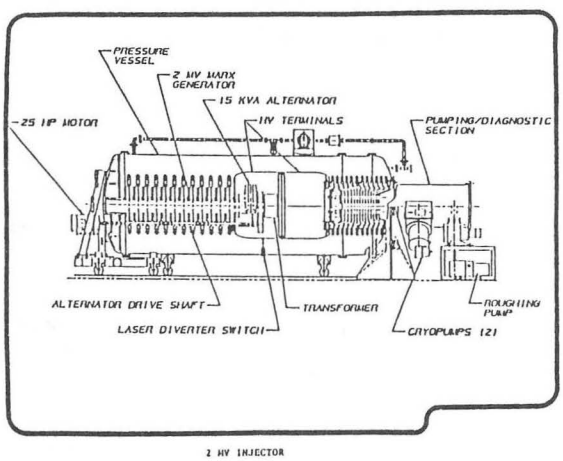

Fig. 1. 2-MV Injector

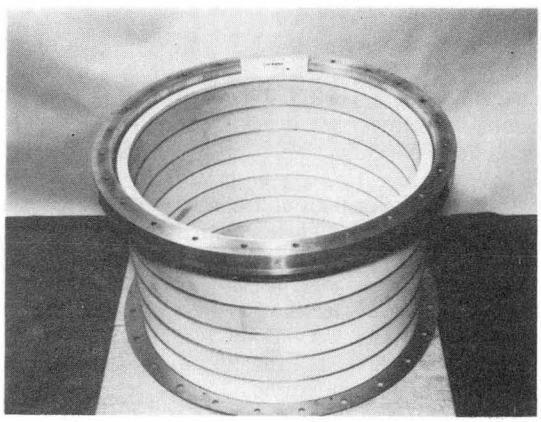

Fig. 2. Ceramic Insulator Module After Etching

CARBON ARC SOURCE DEVELOPMENT

H.L. Rutkowski

A duplicate of the University of New Mexico carbon arc ion source, which is intended for use in the 2 MV injector has been constructed and installed the SBTE. A drawing of the experimental arrangement is shown in Fig. 1. Plasma which is generated at the main arc passes down a drift region to a plasma switch composed of two grids. The second grid is biased negatively with respect to the first grid, causing plasma electrons to be turned back towards the arc. The plasma ions continue on and form a virtual anode very close to the second grid. There is no general plasma flow into the extraction gap because of this plasma switch. At the time when one wishes to extract beam, a high-voltage pulse is applied between the second grid and a grounded extractor electrode. The beam emerges through a hole (2-inch diameter) in this extractor electrode and is diagnosed downstream. The beam exit aperture has a planar 81% transmission grid to prevent blowup of the beam due to penetration of the electric field through the exit aperture. The plasma switch grids are made of the same stainless steel mesh and they also have 2-inch diameter apertures. The cathode for the arc is made of carbon welding rod and it is cylindrical containing the initiating trigger electrode at its center. A surface-flashover plasma from the trigger shorts the main-arc which is powered by a PFN charged to 3 kV and providing 200-A arc current for 100 μsec.

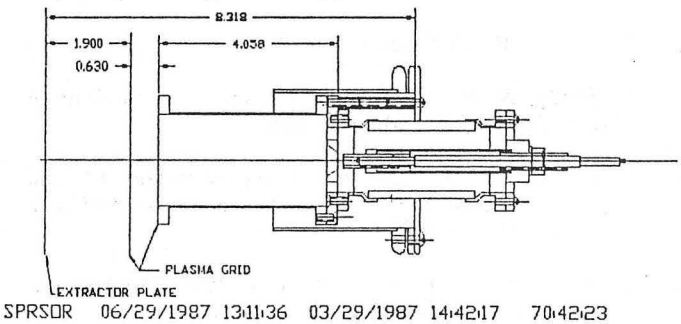

Fig. 1. Carbon arc source, plasms switch, and extractor gap

The beam is diagnosed with a shallow Faraday cup placed 0.5 inches behind the exit aperture with either a 0.125 or 1.0 inch diameter aperture. The same diagnostic paddle contains a .020-inch wide, 2.5-inch long slit for emittance measurements. A slit cup for measuring emittance is located 9.7 inches behind the front slit.

After optimizing the trigger electrode position, the next step is to set the plasma switch voltage. The effect is shown in Fig.2, which shows six-shot overlays of the plasma signal.

Typical extracted beam pulses are shown in Fig.3. The shot to shot scatter is about +/- 10% from the mean value. This may be due to deterioration of the trigger, to cup effects, or to variations in the axial energy of ions produced in the source.

Extracted-beam measurements showed current densities up to 25 mA/cm^2 at 80 kV extraction voltage and good agreement with the Child-Langmuir slope. The current density was below the ideal C-L prediction because of secondary electron production on the cup bias grid. No current saturation was seen or expected because the plasma measurements indicated 93 mA/cm^2 of ions were available at the extraction surface.

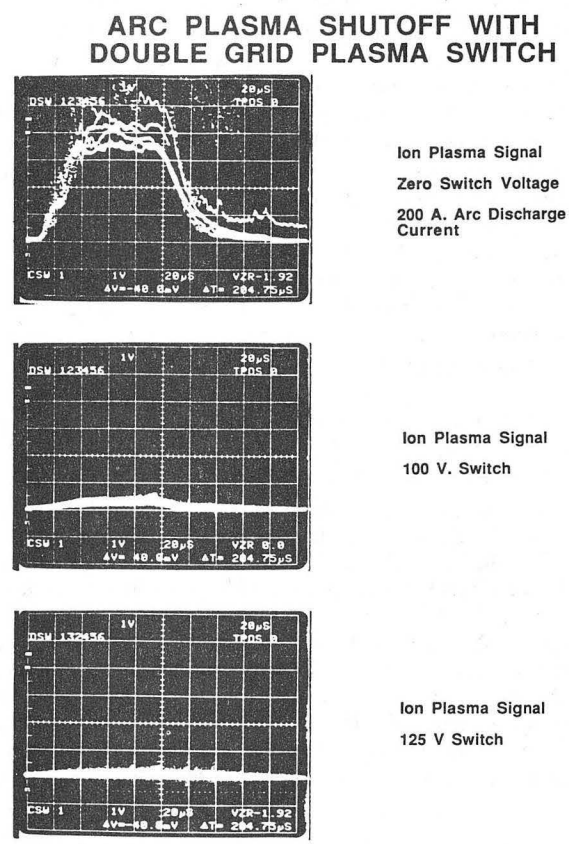

Fig. 2. Raising the bias voltage of the plasma switch shuts off the plasma

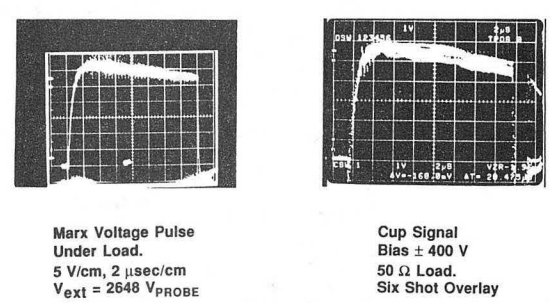

Fig. 3. Typical extracted beam data; 1" aperture shallow Faraday cup.

BEAM COMBINING IN ILSE

David L. Judd

Since the last half-year report increased efforts have been spent on beam combining, with application to ILSE. The example combiner region of successive bends and quads sketched there (Fig. 1) has evolved[1] into an array for combining sixteen beams of C^+ ions at 4 MeV into four. The beam bunches, of duration ~ 1 msec, have head-to tail velocity tilt ~ 20%; therefore either the combiner region must be an achromat or its bending fields must be ramped. Achromatic systems are described elsewhere in this report;[2] they may need both electric and magnetic bending fields, and could use either electric or magnetic quadrupole fields. Such magnetic elements, at locations where they must be very thin between beams, may be of the "sheet-current" type,[3] and may use outer layers of permeable material, as described below Fig. 1 referenced above. Work on designing these elements is described elsewhere[4] in this report.

If the combiner bending fields are to be pulsed they will be electric rather than magnetic. (Design concepts[5] for thin-walled conductor arrays to produce dipole and quadrupole fields are described elsewhere[6] in this report.) A combiner region of this kind is sketched in Fig. 1. It consists of the succession B, F, B, D, -B, F, -B, 1/2D, in which B = bend, -B, = reverse bend, F and D are quadrupoles in an AG lattice, and the final 1/2 D quadrupole serves to produce zero envelope slopes in both x and y at the combiner exit. The nominal occupancy fraction h is 1/2; L = 29.2 cm. For the "stonehenge" geometry, corresponding to the final four-beam pattern in the figure, the transverse displacement shown there is 3.95 cm for d_x and 3.14 cm for d_y. The bending fields are 1.84 and 1.47 MV/m for x and y, with voltages ± 37 and ± 29 kV for electrodes spaced at ± 2 cm. For the same 2 cm, the quadrupole voltages are ± 48 kV.

The best upstream lattice between the injector and the combiner may differ significantly from the lattice just described, but the four quadrupoles indicated may be energized at four different voltages to constitute a matching section between an optimized upstream lattice and the beam envelope properties desired at the combiner exit. It has been found possible to achieve such a match to an upstream lattice having L = 40 cm without requiring excessive quadrupole voltages or beam envelope radii.

References

1. D.L. Judd, "Update on Beam Combining in ILSE," HIFAR Note-165, September 3, 1987.
2. E. Lee, "Acrobatic Beam Combiner for ILSE" this report.
3. D.L. Judd, HIFAR Notes 78 and 79.
4. V. Brady, A. Faltens, and L. J. Laslett, "Quadrupole Magnet Design for ILSE" this report.
5. D.L. Judd, HIFAR Note-162, "Conducting-wire Electric Dipole and Quadrupole Fields for Beam-combining Systems," August 1987.
6. V. Brady, C. M. Celata, and A. Faltens, "Additional Element for Beam Merging" this report.

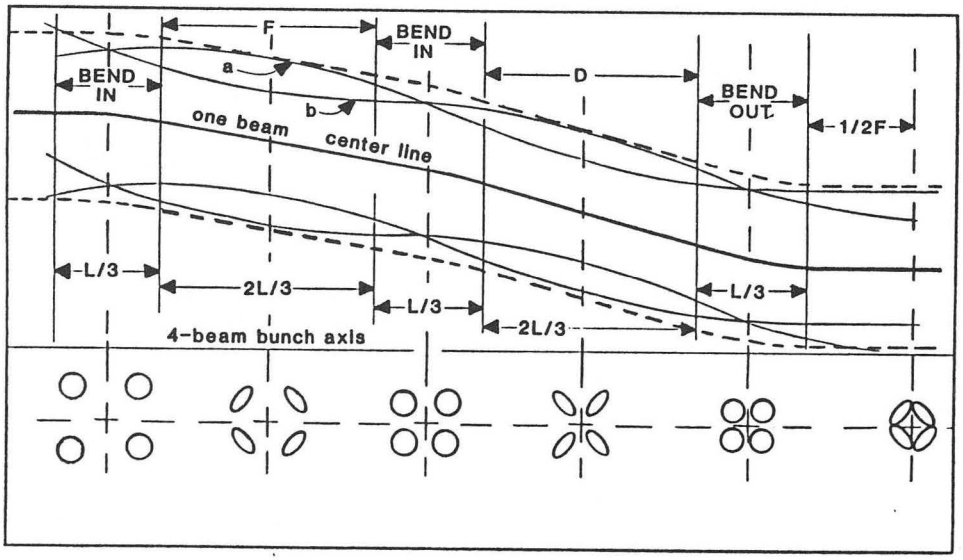

XBL 8611-4313

Fig. 1

EMITTANCE GROWTH DUE TO TRANSVERSE BEAM-COMBINING IN ILSE - ANALYTICAL RESULTS

C. M. Celata

We report here further analytical results of the study of the growth of transverse emittance due to transverse beam combining.

We assume that four identical round beams of uniform density emerge from a "combiner" which bends their orbits so that they finally emerge into a common constant focusing channel. Figure (1) shows the initial geometry. If we assume a final density profile for the combined beam, we can calculate from conservation of energy the final transverse emittance. We assume the final state to be a uniform beam, since simulation shows this to be the case as long as the beams are closely spaced initially. We also assume the initial four-beam configuration to be rms-matched to the focusing system, so that the final beam has the same rms radius as the initial configuration. In matching the final beam, the emittance term in the envelope equation is considered to be negligible compared to the space charge term, so that emittance does not affect the beam radius. Then conservation of energy gives the result:

$$\varepsilon_f^2 = \varepsilon_1^2 \left(1 + 2\frac{\delta^2}{a^2}\right) + \frac{Nq^2}{4mc^2} a^2 \left(1 + 2\frac{\delta^2}{a^2}\right) \left(-\frac{\Delta U}{N^2 q^2}\right) . \qquad (1)$$

where ε_f is the final normalized rms emittance, ε_1 is the initial normalized rms emittance of one beam (rms x-emittance = $\beta\gamma(\langle x^2\rangle\langle x'^2\rangle - \langle xx'\rangle^2)^{1/2}$, and likewise for y), δ and "a" are defined in Fig. (1), N is the number of particles per unit length in the final beam, and ΔU is the change in electrostatic energy from the initial to the final state, or, equivalently, the "nonlinear energy" of the initial state. For the simple geometry of Fig. (1) one can show that

$$\Delta U = \frac{N^2 q^2}{64\pi\varepsilon_0} \left\{ 3 - 4 \ln \left[\frac{1-g^8}{4} \left(\frac{a}{\delta}\right)^3 \left(1 + 2\frac{\delta^2}{a^2}\right)^2 \right] \right\} \qquad (2)$$

where g is δ/R, and R is the pipe radius. Note that since $g^8 \ll 1$, $\Delta U/(N^2 q^2)$ is essentially a function of one parameter, δ/a.

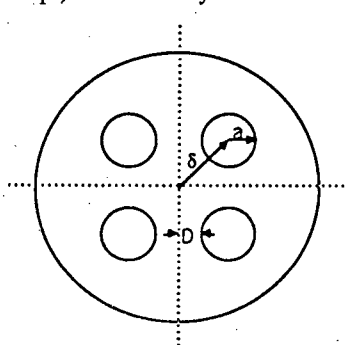

Fig. 1. Initial beam configuration.

The first term in Eq. (1) is equal to the so-called "geometric" increase in emittance, which represents the increase in rms emittance of the four-beam initial configuration over that of a single beam. The second term gives the increase in emittance due to space charge, and is due to the conversion of electrostatic field energy to transverse kinetic energy as the beams mix. For the space-charge-dominated beams of interest, ε_1 is very small, and the second term in Eq. (1) dominates. Using the fact that for a uniform round beam in a constant focusing system $N_1 q^2/(2m\langle v_x^2\rangle) = (\sigma_0^2 - \sigma^2)/\sigma^2$, where N_1 is the number of particles per unit length for one of the initial beams, one can express the ratio of the two terms in the simple form

$$\frac{\Delta}{\varepsilon_1^2 \left(1 + 2\frac{\delta^2}{a^2}\right)} = 8 \left(-\frac{\Delta U}{N^2 q^2}\right) \frac{\sigma_0^2 - \sigma^2}{\sigma^2} . \qquad (3)$$

where Δ is the second term in Eq. (1). Though the space charge term dominates, for δ/a near its minimum value of $\sqrt{2}$ it can not be assumed that the geometric term is negligible.

We are particularly interested in the case of constant D (see Fig. 1), since space taken by hardware in ILSE will dictate some fixed minimum distance between the edges of the beams when they first emerge from the combiner. Fig. (3) shows $\Delta^{1/2}$, the final emittance if ε_1 can be neglected, vs δ/a. Since $\delta/a = \sqrt{2}\,(1+D/a)$, Δ can be written, using Eq. (2), as $Nq^2D^2/(4mc^2)$ times a function of a/D alone. It is therefore trivial to scale the results of Fig. (3) to other values of D, N, or q. We expect $Nq \approx 0.4\mu C/m$ in ILSE, for a beam of C^+. Fig. (2) predicts that the emittance growth due to combining will be acceptable, i.e., it will not unduly impair the ability to focus the beam onto a spot.

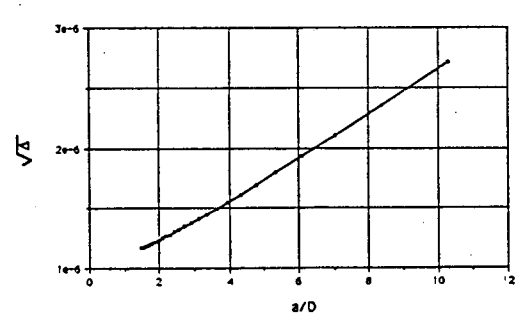

Fig. 2. $\Delta^{1/2}$ vs. a/D. D = 3 mm; Nq = 0.4 μC/m, charge state = +1, atomic weight = 12.

The analytical formulae given above have been extremely useful in predicting qualitative scaling of emittance growth with lattice and beam parameters. However, because the geometry in the ILSE experiment will be quite different from Fig. (1) (See "Transverse Beam Combining in ILSE--Particle Simulation Results" in this report), only rough quantitative agreement (to a factor ~ 2) is seen with particle-in-cell simulations of the experimental geometry. The transverse particle-in-cell simulation SHIFTXY has been used to check the analytical results for the geometry of Fig. (1). It shows agreement with the formulas given.

Reference

1. C.M. Celata, A. Faltens, David L. Judd, L. Smith, and M.G. Tiefenback, "Transverse Combining of Nonrelativistic Beams in a Multiple Beam Induction Linac", presented at the Particle Accelerator Conference (Washington, D.C., March 1987), to be published as IEEE Proceedings.

TRANSVERSE BEAM COMBINING IN ILSE -- PARTICLE SIMULATION RESULTS

C. M. Celata

In this report we summarize the results of particle-in-cell simulations of transverse beam combining in ILSE performed with the two-dimensional PIC code SHIFTXY. We assume that the beams, which were individually focused upstream of the combining system, have been moved closer together by dipoles in the combiner, and emerge into a common focusing channel whose transverse boundary is a round conducting pipe. The simulation follows them from this point. Linear focusing forces in an alternating-gradient arrangement have been assumed. The initial <x> and <y> of the distribution, measured about the center of the focusing channel, are zero. Image forces due to charge induced on the boundary are computed self-consistently. The beams initially are assumed to be identical, with uniform density. The velocity distribution is Maxwellian, with uniform temperature given by the initial emittance. The geometric arrangement of the beams when they first emerge from the combiner (i.e., the initial spatial distribution for the simulation) will be discussed below. The quantity of most interest is the subsequent transverse emittance growth, but it is also necessary to consider the size and oscillations of the "beam" envelope. Note that since the beam distribution function is evolving in time and does not in general have elliptical symmetry, the usual rms envelope equation does not apply. In the cases described below, the rms envelope equation has nevertheless been applied, as an approximation, to attempt to match the initial beam configuration to the focusing lattice. This is quite successful, as measured by the amplitude of oscillation of the rms envelope radii, for the beam spacings of interest.

Initial Beam Configuration

Because they share focusing electrodes in the electrostatic lattice, neighboring beam shapes in ILSE will differ by a 90° rotation. Two initial beam configurations for combining were identified for this situation, the "symmetric" and "stonehenge" geometries (see Fig. (1)). Simulation studies for these two configurations showed that more emittance growth occurred for the symmetric configuration, as expected, because the beams are not as closely packed as in the stonehenge geometry.

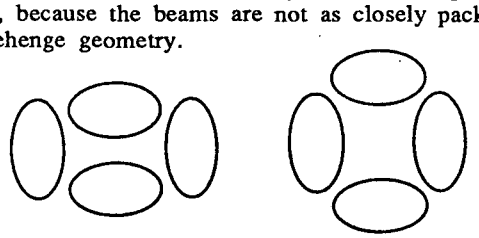

Fig. 1. Possible initial configurations of four beams as they emerge from the combiner into a common focusing channel. "Stonehenge" (left) and "symmetric" (right) configurations.

The stonehenge geometry also has the advantage that since the rms x and y radii of the configuration are not equal, this arrangement of beams can be rms-matched to the downstream focusing channel. The symmetric geometry, on the other hand, will cause a large mismatch in the final beam.

Figure (2) shows the time history of the emittance and of xrms for the stonehenge configuration with the minimum distance between beam edges equal to 5.2 mm. [This interbeam distance represents a conservative guess-- the beams might be as close as 3 mm in ILSE.] The downstream lattice half-period was assumed to be 40 cm, and σ_0 before and after combining was 63°. $2\langle x^2\rangle^{1/2}$ for the initial configuration was set equal to 75% of the aperture. The charge per unit length used was 0.09 μC/m per initial beam; the beam energy was 4 MeV; the initial normalized rms emittance of each beam was 1.45 x 10^{-7} m-rad in each transverse plane; and the ion assumed was C^+. The initial configuration was rms-matched to the downstream focusing lattice, using an equivalent uniform beam (same total charge and rms radii as the initial distribution). As seen in the figure, there is an initial fast rise of emittance, as described by Wangler[1] for the evolution of nonuniform beams, of which this is an extreme example. The emittance then falls. Oscillations of the emittance thereafter are small, and damp away by about the 30th lattice period following the combiner. The decreases in rms emittance seen periodically in Fig. (2) seem correlated with a loss of a small number of particles (2% over 50 periods). Though phase plots show that the emittance growth in Fig. (2) is not simply due to a small minority of particles in a halo, the details of the distribution function have not yet been investigated. The rms envelope in x (and also in y) is well-behaved, with an oscillation of about 5%. Since the initial configuration was matched to the focusing channel without considering the rise in emittance during beam mixing, it is possible that this small oscillation in xrms could be eliminated with proper tuning of the experiment.

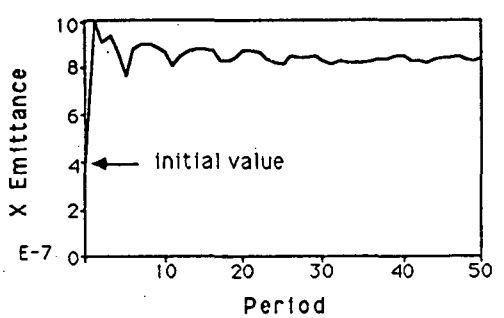

Fig. 2. Normalized rms emittance in the x plane, and xrms vs z for the parameters given in the text.

The above simulation was done for conditions at the longitudinal center of the beam. The beam head and tail will be moving slower (faster) than the center, and therefore the radii of the initial beams at these locations will be different from that at the center. Assuming the combiner to be achromatic, however, the transverse centroid of each of the four beams will be at the same transverse position for every longitudinal position along the pulse. Therefore the interbeam spacing will be different at different longitudinal positions, causing the emittance growth to be different. Simulations of the head, tail, and center for the case shown in Fig. (2) (interbeam spacing at the center of 5.2 mm, and 3.8 mm at the tail, 6.6 mm at the head) show emittance growth of the head to be 23% larger than the beam center, and the tail to be 5% smaller.

Reference

1. T. P. Wangler, K. R. Crandall, R. S. Mills, and M. Reiser, IEEE Trans. on Nuc. Sci., NS-32, 2196 (1985).

ACHROMATIC BEAM COMBINER FOR ILSE

Ed Lee

Until recently the lattice designs considered for beam combining in ILSE[1] consisted of a short series of electrostatic quadrupoles and electric or magnetic bends (typically a total of 6-8 elements per beam). Groups consisting of four beams each are translated onto parallel trajectories separated by only a few centimeters. While this type of configuration is efficient in cost and total length, it is not intrinsically achromatic. That is, because of the expected velocity tilt of ±10% the beam head and tail will be directed onto trajectories removed from the design orbit by ~±4 mm and deviate from the parallel by ~±1.5 mr. These are unaccceptably large variations, resulting in beam loss and emittance growth. One method for removing these first order chromatic effects consists of ramping the bends (and possibly the quadrupoles) during passage of the beam such that the entire pulse follows the design orbit of the central portion. The main difficulties with this scheme are the extra costs associated with control of wave forms, and the relatively large amount of stored field energy which must be supplied over the pulse duration ($\tau_p \sim 1\ \mu s$).

In view of the anticipated difficulties of rapidly ramped waveforms, a second approach to the chromatic problem has been recently pursued. If sufficiently long combiner systems are permitted (twelve or more elements), then arrangements of quadrupoles and bends can be found which are intrinsically achromatic through first order in $\Delta v/v_0$. No field ramping is required except to avoid overheating of magnets; this can be applied on a time scale of several ms. The essential property of the achromatic designs is that the trajectory of a portion of the pulse with momentum different from the design value, while it deviates from the design trajectory, coincides with it in position and direction at the end of the combiner.

A variety of achromatic designs are being examined. The shortest such systems are the most complex in that they involve both electric and magnetic bends and their fields are relatively high (B ~ 0.4 T, E ~ 15 kV/cm). Longer systems can be made entirely with electrostatic bends and quadrupoles. In the longest design considered (six full focal periods) only two very weak bends are required in addition to the quadrupoles. In this case it appears that the elements may be made to simultaneously bend and focus the beams (combined function). This would leave ample room for diagnostics, pumping, etc. between the quadrupoles, and acceleration could also be applied if desired.

A much shorter system consisting of three focal periods has also been studied. It uses magnetic bends near the entrance and exit of the combiner to deflect the design orbit to the desired offset and straighten it. Four electric bends are used in the intermediate zone to correct the momentum dispersion, producing an achromat at the system end. This combiner is only half the length of the six-period device, but its magnetic bend fields are higher by a factor of four. Dispersion plots for this system are given in Fig. 1 (images absent) and Fig. 2 (images present).

Reference

1. C.M. Celata, A. Faltens, David L. Judd, L. Smith and M. Tiefenback, "Transverse Combining of Nonrelativistic Beams in a Multiple Beam Induction Linac," abstract submitted to the 1987 Particle Accelerator Conference, March 16-19, 1987, Washington, D.C.

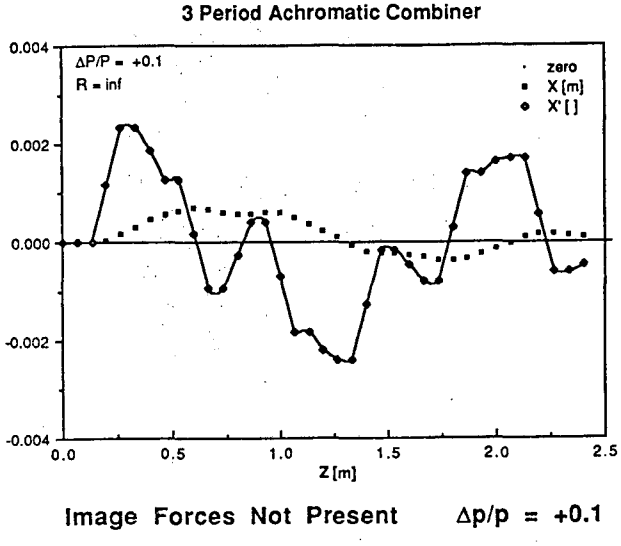

Fig. 1. The centroid amplitude x (dispersion) and angle x' are displayed as a function of distance measured along the centerline of the three period achromat for a momentum deviation $\Delta p/p_0 = +0.1$. Image forces are not computed.

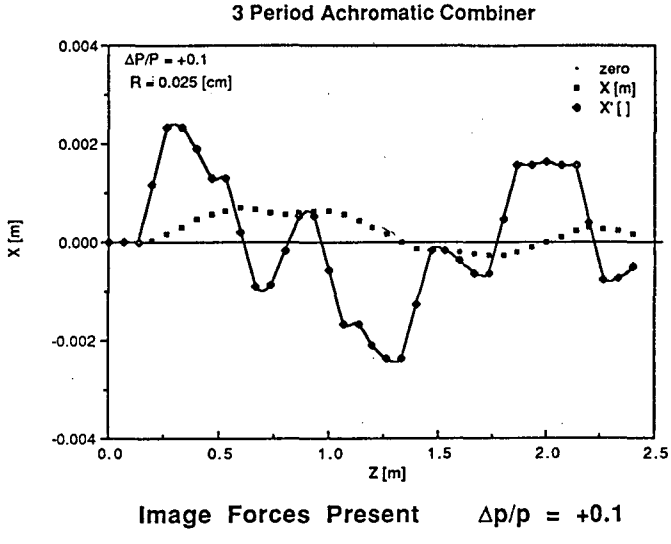

Fig. 2. The centroid amplitude and its derivative are displayed for a system identical with that of Fig. 1, but with image forces taken into account.

ADDITIONAL ELEMENTS FOR BEAM MERGING

V. Brady, C.M. Celata, A. Faltens

The computational results for emittance growth due to merging of four beams into one which were reported at the 1987 PAC Conference were based on an assumed beamlet to beamlet separation of 3 mm. These results were acceptable for applications such as ILSE and future drivers. Subsequent examination of some of the candidate element geometries, beam clearances, and beam halos achieved in the SBTE beam indicated that the separation for a conservative design could increase beyond 1 cm. Because the increase in emittance is almost linearly proportional to the beamlet separation for a space-charge dominated process, several changes were instituted to decrease the separation. In ILSE the merging would take place after the beam has passed through only about 40 focusing lenses, leading to a negligble 0.5 mm transverse misalignment with typical tolerances, and the beam halo would be about 1 mm. By making beam bending and focusing elements which are very thin between the beamlets to be merged, and by scraping off the beam halo in these elements or immediately before them, we can approach the initially assumed beamlet separations.

Two new types of final combining elements have been investigated: multi-electrode "squirrel cages" for electric dipoles and quadrupoles, and multi-wire current distributions within iron boundaries for magnetic dipoles and quadrupoles. Both these types of elements are based on starting with the desired multipole, drawing in the desired close-fitting boundary about the beamlets to be merged, and calculating the potential distribution or current distribution on that boundary for the multipole (or combination of multiples if desired). The ideal distributions are then approximated by a discrete number of electrodes or conductors, for which the minimum number is determined by the decay of near-field aberrations in the direction of the beam and the maximum number by practical considerations such as deflection of very fine electrodes in the electric field and resistive heating of very fine wires.

The electric elements are more suitable for merging scenarios where it is necessary to change the fields significantly during the 1 microsecond beam pulse, but would have some risk of electrical breakdown due to the anticipated scraping off of the halo. The magnetic elements are better matched to the achromatic systems which can operate with fixed fields during the pulse, although they too would be pulsed on a millisecond time scale to permit use of small, uncooled conductors carrying typically several hundred amperes. An example of the magnetic quad array is shown in Fig. 1, and an example of the magnetic dipole array is shown in Fig. 2. Both of these examples are based on obtaining single-particle angular errors which are small compared to the errors that are expected from the merging. The actual geometries would be updated as the entire system design advances.

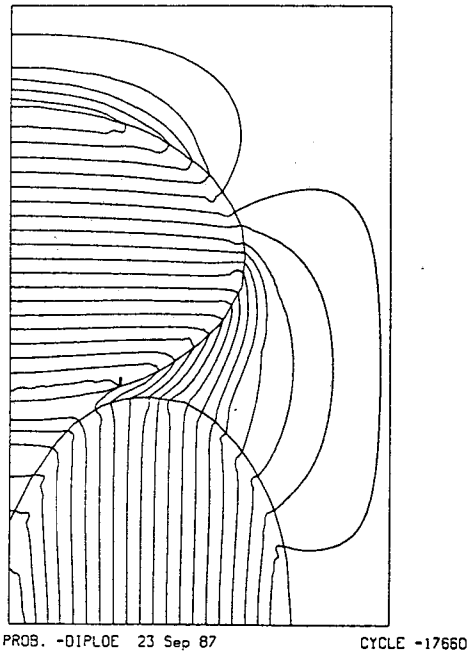

Fig. 1. Field lines in an iron yoke four-beam quadrupole array used as the last element in the merging section. The ~ 1 mm diameter conductors shown are the minimum number that would produce acceptable fields over the beams, which would fill the aperture to within 1-2 mm of the surrounding iron boundary.

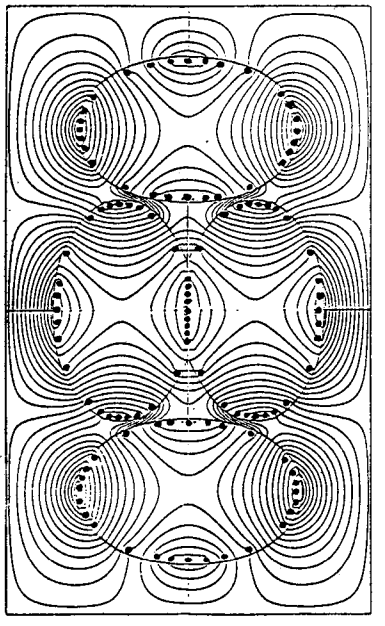

Fig. 2. Field lines in one quadrant of a four-beam iron-yoke dipole array. As in the quad array of Fig. 1, a very thin iron septum beween beams is sufficient for redirecting the external field from one aperture into the next one.

QUADRUPOLE MAGNET DESIGN FOR ILSE

V. Brady, A. Faltens, L.J. Laslett

During the past nine months several magnetic quadrupole lens designs have been generated and examined for possible application in the ILSE experiment. These designs were carried to various states of completion as problems became apparent with the design or the machine parameters changed. Some of these designs will be reviewed very briefly, leading up to the present work-in-progress.

The initial design which was considered was a standard dc-powered quadrupole which had its fields determined by the shape of the iron poles -- that is, an "iron-dominated" design. Detailed examination showed that the desired specifications at that time could be met by such a design, but that the cross sectional area of the conductors in each quadrant of the magnet would have to be of comparable size to the aperture if conventional water-cooled conductor current-density limits were accepted. This was a consequence of the unfavorable scaling which results if a given aperture is scaled to smaller dimensions, wherein the conductors realistically must take a larger fraction of the overall cross section as the magnet is scaled down. For a multiple-beam array the consequence was that the beams would have to be spaced an undesirably large distance from each other, resulting in increased sizes and costs in the entire induction accelerator.*

The next iteration was to change to a pulsed system, which would allow the conductor current densities to be greatly increased. Assuming that the cost for such a design is proportional to the pulsed energy which must be supplied to the magnet from a capacitor bank, one can find a balance between (i) the energy stored in the volume occupied by the conductors and the now-increased insulation, and (ii) the energy dissipated in the conductors, core laminations, and induced eddy currents, which minimizes the energy and the cost. This results in a conductor package about 1-cm deep by 4-cm wide and a current pulse which is approximately a 1-millisecond half-sine. These designs were pursued to the point of determining the iron yoke requirements and the influence of adjacent magnets on each other. The spacing between beams, or the "pitch", decreased to almost half of the pitch of the initial design.

A design option with a pulsed quad is the use of a large number of smaller conductors, because cooling is by conduction to the outside rather than by internal water channels. This option makes practicable a current-dominated design, which is the preferred choice at this time. By accurate placement of the conductors around the inner boundary of a circular iron yoke, a satisfactory field distribution may be obtained and the pitch reduced further. This option is also desirable for correctly treating the end effects of the quadrupole. The solution of the end effect problem has wider application than just to ILSE, because it directly relates to the maximum bore-to-length and bore-to-half-period ratios which may be attained and which limit the transportable current at the low energy end of similar machines such as HIF drivers.

Consideration accordingly has been given to designs in which the undesired higher harmonics of the quadrupole are suppressed in the integral sense. In the interest of axial compactness, the end windings are placed in the form of circular arcs developed by sharp 90-degree bends at the ends of the straight portions of the windings. The end windings may be stacked as close to one another as the wire thickness permits, and the angular portions of the straight windings then are adjusted to suppress certain harmonics (with respect to θ) of the integral of the z-component of the current with respect to z. These results are given in HIFAR Note-147 by V. Brady. The iron yoke thickness for this design is just sufficient to shield adjacent beams from each other. The iron yoke in these designs extends axially far enough beyond the windings to allow the free-space calculations to be good descriptions of the fields except for an increase in the magnitude of the field due to the presence of the iron. A four-beam array of these quadrupoles, suitable for transport of the ILSE beams after merging, is shown in Fig. 1.

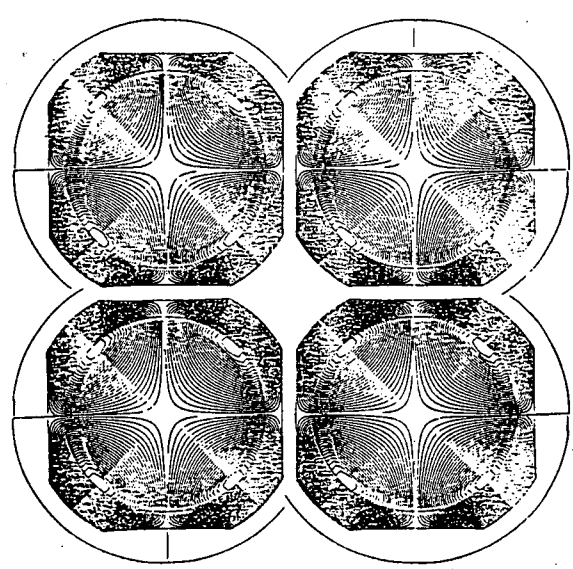

Fig. 1. A four-beam pulsed magnetic quadrupole array.

---

*The use of superconducting magnets, as would be adopted ultimately in a driver design, of course would remove the restrictions mentioned.

WAVEFORMS AND LONGITUDINAL BEAM-PARAMETERS FOR ILSE

D. Keefe and C. Kim

We summarize here results for a reference design, named "ILSE-30," of an acceleration schedule for ILSE based on computations made with the SLID code. ILSE poses some difficult problems in this regard. The first stems from the choice of a light ion (carbon) for the experiment. The initial bunch length entering the accelerator from the 2-MV injector is ℓ = 6.8 meters. The overall length of the accelerator -- 36 meters -- is thus not very long compared with ℓ, viz. 5 ℓ. It is difficult to accomplish significant bunch-length shortening in so short an accelerator, without appealing to extremely large values of the head-to-tail velocity-shear, $\Delta\beta/\beta$. (By contrast, MBE-4 has a length 18 ℓ, and a driver a length ~ 200 ℓ.) A somewhat shortened bunch-length, L, at the end of the accelerator is desirable to keep the final drift-compression beam length, $L/(\Delta\beta/\beta)_f$ to a manageable scale.

The second problem arises from the constraints on $\Delta\beta/\beta$ that must be observed at (a) the location of the 4-to-1 beam combiners, and (b) the exit of the accelerator where the 180° bend occurs. Achromaticity in each of these manipulations requires $(\Delta\beta/\beta)_c < 0.2$ at the combiner, and $(\Delta\beta/\beta)_f < 0.12$ at the bend. The ILSE-30 design comes close to meeting these conditions, with $(\Delta\beta/\beta)_c = 0.21$, and $(\Delta\beta/\beta)_f = 0.127$ The pulse length ratio is $L/\ell = 0.84$.

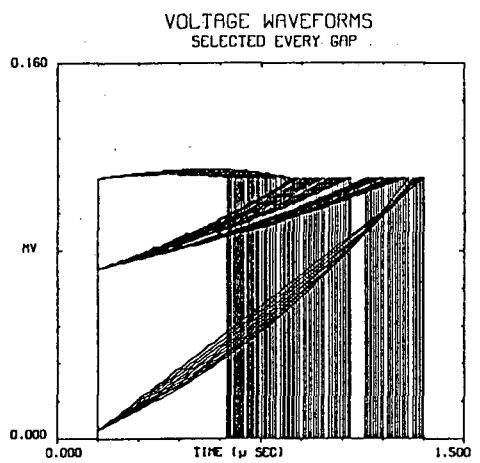

Fig. 1. The initial and final intervals of 150 nsec are not shown; the waveforms in these intervals (so-called "ears") will be chosen to contain the steep rise and fall of the bunch ends.

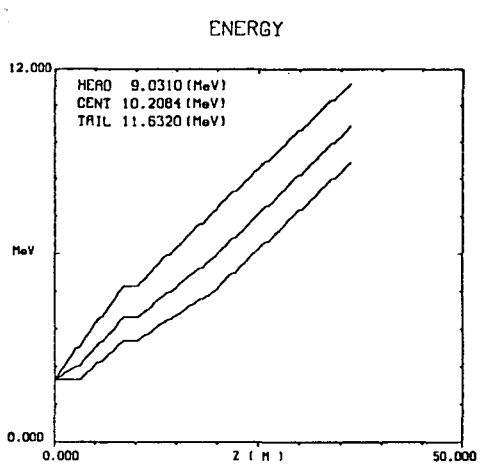

Fig. 2. Note that acceleration of the bunch head does not start until z = 3 m (when $\Delta\beta/\beta$ has risen to its constrained value, 0.21). Also, acceleration does not occur at the combiner (z = 8 to 10 m) and at the short diagnostic sections introduced at 10-gap intervals.

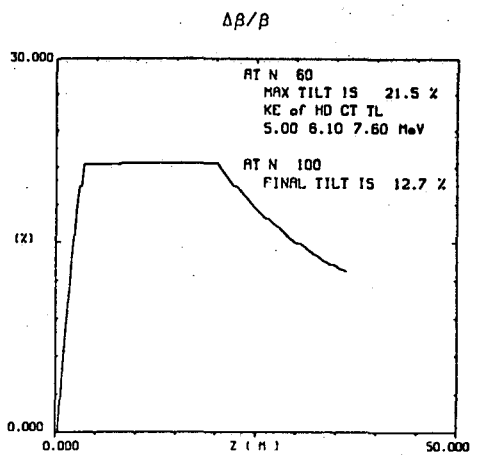

Fig. 3. $\Delta\beta/\beta$ is brought rapidly to the maximum value of 0.21 until the 6 MeV point whereafter it falls off as 1/E to reach a value $(\Delta\beta/\beta)_f = 0.127$ at the 10 MeV point.

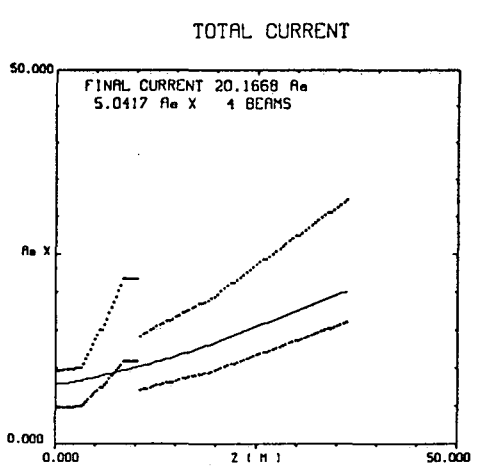

Fig. 4. The "fill-factor" of the beam (beam radius/aperture radius) can be gauged by comparison with the dotted curves; the upper one corresponds to a 70% fill-factor, the lower to 50%.

PUBLICATIONS AND INTERNAL NOTES

HIFAN-321
LBL-21194
Fessenden

T.J. Fessenden, C.M. Celata, A. Faltens, T. Henderson, D.L. Judd, D. Keefe, L.J. Laslett, J. Meneghetti, C. Pike, D. Vanecek,
"Preliminary Design of A ≈ 10 MV Ion Accelerator for HIF Research," Presented at the Second International Topical Symposium on ICF Research by Particle Beams, Nagaoka, Japan, June 16-18, 1986, Laser and Particle Beams (1987), vol. 5, part 3, pp. 457-463.

HIFAN-362
LBL-23168
HIFAR Staff

HIFAR Staff,
"Heavy Ion Fusion Accelerator Research (HIFAR) Half-Year Report, October 1, 1986 - March 31, 1987," HIFAN-362, LBL 23168.

HIFAN-363
Hovingh

J. Hovingh,
"Heavy Ion Fusion Meeting: Topic: Accelerator Costs, Friday, March 13, 1987," March 27, 1987.

HIFAN-364
Lee

E. P. Lee,
"Dynamics of Heavy Ion Beams During Longitudinal Compression," 1987 IEEE Particle Accelerator Conference, Washington, D.C., March 16-19, 1987.

HIFAN-365
LBL-21523
Krafft

G. Krafft,
"Collective Focusing of Intense Nonrelativistic Ion Beams by Co-Moving Electrons," Ph.D. Thesis, University of California, Berkeley, April 1987.

HIFAN-366
LBL-23015
Anderson

O.A. Anderson,
"Emittance Growth in Expanding Charged Beams," submitted to *Particle Accelerators* March 24, 1987.

HIFAN-367
Bangerter

R. Bangerter & D. Keefe,
"Conference and Symposia: Heavy Ion Fusion," Report on the International Symposium held at Washington, D.C. May 27-29, 1986.

HIFAN-368
Ho

D-M. Ho, R. Bangerter, E.P. Lee, and S. Brandon,
"Lonitudinal Compression of Heavy-Ion Beams with Stringent Requirements on Final Focus," April 1987.

HIFAN-369
Bangerter

R. Bangerter, D-M. Ho, B. Langdon, E.P. Lee, and K. Levedahl,
"Target Charging and Photo-Ionization of Background Gas," DOE Heavy Ion Fusion Review, Berkeley, CA, April 9-10, 1987.

HIFAN-370
Ho

D-M. Ho, R. Bangerter, E.P.Lee, S. Brandon, and J.W-K. Mark,
"Dynamics of Heavy Ion Beams During Longitudinal Compression," submitted to the 1987 IEEE Particle Accelerator Conference, Washington, D.C., March 16-19, 1987.

HIFAN-371
LBL-23326
Keefe

D. Keefe,
"Status of Inertial Fusion," Panel Discussion on Status of Inertial Confinement Fusion at the Fusion Power Associates Annual Meeting and Symposium, Applications of Laser, Particle Beam and RF Power Technologies, Pleasanton, CA, April 8-9, 1987.

HIFAN-372
LBL-23772A
Kim

C. Kim & D. Keefe,
"Acceleration Schedules and Beam Parameters in the Induction-Linac-System Experiment," abstract submitted to the Twenty-Ninth Annual Meeting, Division of Plasma Physics, November 2-6, 1987.

HIFAN-373
LBL-23772A
Celata

C.M. Celata, A. Faltens and D.L. Judd,
"Transverse Combining of Beams in the Proposed ILSE Experiment," abstract submitted to the Twenty-Ninth Annual Meeting, Division of Plasma Physics, November 2-6, 1987.

HIFAN-374
LBL-23772A
Lee

E.P. Lee, A. Faltens, and D.L. Judd,
"Achromatic Configurations for Beam Combining in the Proposed ILSE Experiment," abstract submitted to the Twenty-Ninth Annual Meeting, Division of Plasma Physics, November 2-6, 1987.

HIFAN-375
LBL-23772A
Rutkowski

H.L. Rutkowski, A. Faltens, D. Brodzik, and D. Vanecek,
"Progress of Carbon Arc Souce Development for a Heavy Ion Fusion Injector," abstract submitted to the Twenty-Ninth Annual Meeting, Division of Plasma Physics, November 2-6, 1987.

HIFAN-376
LBL-23772A
Meuth

H. Meuth, T.J. Fessenden, D.E. Gough, C.H. Kim, C.D. Pike, and D. Vanecek,
"Progress on the MBE-4 Multiple-Beam Ion Induction Accelerator," abstract submitted to the Twenty-Ninth Annual Meeting, Division of Plasma Physics, November 2-6, 1987.

HIFAN-377
LBL-23748
Anderson

O.A. Anderson, W.S. Cooper, W.B. Kunkel, C.F. Chan, L. Soroka, C.H. Kim, A.F. Lietzke, C.A. Matuk, P. Purgalis, and R.P.Wells,
"Accelerator and Transport Systems for High-Current Negative-Ion Beams," IAEA Technical Committee Meeting on Negative ion Beam Heating, Culham Laboratory, July 15-17, 1987.

HIFAN-378
Keefe

D. Keefe,
"Foreign Trip Report,
June 29 - July 4, 1987: ECFA Workshop on New Developments in Particle Acceleration Techniques;
July 6 - 7, 1987: Visits to Laboratories in Paris Area,"

HIFAR NOTES (Internal and Informal)

HIFAR Note-137
Brodzik

D. Brodzik,
"ILSE/Integrated Controls," May 18, 1987.

HIFAR Note-138
Brady

V. Brady,
"Current Filament Quadrupoles for ILSE," March 25, 1987.

HIFAR Note-139
Kim

C. Kim,
"An ILSE Physics Design," April 1, 1987.

HIFAR Note-140
Hovingh

J. Hovingh,
"LANL Module Investigation Project," April 23, 1987.

HIFAR Note-141
Hovingh

J. Hovingh,
"Comparison of the Unit Cost Distributions of an Accelerator Design Using 1985 Costs with 1979 Costs," May 7, 1987.

HIFAR Note-142 (Cancelled).

HIFAR Note-143
Brady

V. Brady
"MBE-4: Harmonics of the Quadrupole Potential and of the Image-Field Potential of the Electrodes," May 8, 1987.

HIFAR Note-144
Keefe

D. Keefe,
"Towards a Self-Consistent ILSE Reference Design," May 14, 1987.

HIFAR Note-145
Brady

V. Brady,
"2-D Dipole Windings," May 1987.

HIFAR Note-146
Brodzik

D. Brodzik,
"Carbon Arc, Single Beam Source Modifications," April 1987.

HIFAR Note-147
Brady

V. Brady,
"12 Wire 3-D Dipole," May 21, 1987.

HIFAR Note-148
Laslett

L.J. Laslett,
"Illustrations of the Effect of an Abrupt Change of Half Period for a Magnetostatic Transport Lattice," June 1, 1987.

HIFAR Note-149
Kim

C. Kim,
"ILSE Design Progress Report," June 4, 1987.

HIFAR Note-150
Judd

D. Judd,
"Simple Estimates on Avoiding Mismatch Due to a Lattice Period Change," June 9, 1987.

HIFAR Note-151
Hovingh

J. Hovingh
"Approximate Velocity Tilt Limits for LIACEP," June 11, 1987.

HIFAR Note-152
Judd

D. David
"Beam-Combining in ILSE," June 11, 1987.

HIFAR Note-153
Lee

Edward Lee,
"Achromatic Beam-Combining in ILSE," June 18, 1987.

HIFAR Note-154
McCreight

S.H. McCreight,
"Seminar: Coding for Data Acquisition on MBE-4," July 9, 1987.

HIFAR Note-155
Celata

C. Celata,
"Beam-Combining and Magnetic Transport in ILSE," June 1987.

HIFAR Note-156
Lee

E.P. Lee,
"Three-Period Achromatic Beam-Combining in ILSE," July 24, 1987.

HIFAR Note-157
Lee

E.P. Lee,
"Electrostatic Beam-Combiners," July 30, 1987.

HIFAR Note-158
Kim

C. Kim,
"ILSE Design Parameter Update," August 5, 1987.

HIFAR Note-159
Celata

C. Celata,
"Continued Deliberations on Beam-Combining in ILSE," August 6, 1987.

HIFAT Note-160
Fessenden

T. Fessenden, C. Kim, H. Meuth, H. Rutkowski,
"Physics Progress on MBE-4 and SBTE since the April 1987 Review," Augut 11, 1987.

HIFAR Note-161
Brady

V. Brady,
"Current-Dominated Quadrupole for ILSE," August 12, 1987.

HIFAR Note-162
Judd

David Judd,
"Conducting-Wire Electric Dipole and Quadrupole Fields for Four-Beam Combining Systems," August 1987.

HIFAR Note-163
Faltens

A. Faltens,
"Special Elements for Beam Combining," August 14, 1987.

HIFAR Note-164
Lee

E.P. Lee,
"Return to Achromatic Combiner," September 3, 1987.

HIFAR Note-165
Judd

D. Judd,
"Update on Beam Combining in ILSE," September 3, 1987.

HIFAR Note-166
Fessenden

T. Fessenden,
"An Estimate of the Beam Deflection Within the MBE-4 Gun," September 21, 1987.

HIFAR Note-167
Laslett

L.J. Laslett,
"Fields of a Provisional Downstream Magnetic Quadrupole for ILSE - Part I," September 1987.

HIFAR Note-168
Laslett

L.J. Laslett,
"Fields of a Provisional Downstream Magnetic Quadrupole for ILSE - Part II," September 1987.

HIFAR Note-169
Hovingh

J. Hovingh,
"Superconducting Quadrupole Costs from LIACEP Output," October 1987.

HIFAR Note-170
Laslett

L. J. Laslett,
"Image Fields in the Beam Combiner," August 1987.

H.I.F. STAFF ROSTER

Denis Keefe

Donald A. Brodzik
Warren Chupp
Robert D. Edwards
Andris Faltens
Thomas J. Fessenden
Ron Gervasoni
William B. Ghiorso
David Gough
Wayne Greenway
Ralph Hipple
Cai Houston
Charles H. Kim
David Jerko
Bruce MacDonell
John Meneghetti
Hermann Meuth
Harry Meyer
Joseph Perez
Chester D. Pike
Thomas Purtell
James Rice, Jr.
Henry L. Rutkowski
Gerald L. Stoker
Bill Tiffany
David Vanecek
A.I. Warwick
Gerald West
John Yeager, Jr.
Marco Zbinden

Lloyd Smith

Victor Brady
Christine Celata
Elon Close
David L. Judd
L. Jackson Laslett
Edward P. Lee

William B. Herrmannsfeldt, SLAC

Jack Hovingh, LLNL

HALF-YEAR/YEAR-END REPORT: DISTRIBUTION LIST

Allied Chemical Corporation

Carl Smith

Argonne National Lab.

Thomas A. Fields
Ronald Martin

University of Arizona

R. Morse

Batelle

John Hartman

BMD/ATC/SDC

Milton Hawie
Brian Strickland

Brookhaven National Laboratory

Mark Barton
E. Courant

C.E.A. Bruyeres-le-Chatel

R. Dei-Cas

CEBAF

J. Bisognano
D. Douglas
H. Grunder
G. Krafft
C. Leemann

University of Calif., Irvine

Norman Rostoker

Cornell University

John Nation
Ravi N. Sudan

DARPA

H. Lee Buchanan

Department of Defense (SDIO)

Richard Gullickson
W. Higgins

Department of Energy

DP-OIF

Gregory D'Alessio
Sheldon L. Kahalas
R. Schriever
Marshall Sluyter

ER

Ryszard Gajewski (AEP)
Gerry Peters (HENP)
Walter Polansky (AEP)
Robert Rader (OPA)
D. Stevens (BES)
David F. Sutter (HENP)
James Decker, Dir.,
Office of Energy Research
W. Wallenmeyer (HENP)

DOE San Office

Rudolf Bredderman
Dennis Neely

E.P.R.I.

Robert Scott

Fermi National Accelerator Lab.

Frank T. Cole
Fred Mills
Lee Teng

F.O.M. Amsterdam

F. Siebenlist

GANIL

P. Lapostolle

GE

John Lucek

GSI

R. Bock
D. Boehne
I. Hofmann

Univesity of Illinois

G. Miley

Institute for Nuclear Study

Y. Hirao

KMS Fusion, Inc.

Alex Glass

Kanazawa University

S. Kawasaki

Lawrence Berkeley Laboratory

D. Attwood, 80/101
R. Avery, 46/189
K. Berkner, 50/149
D. Brodzik, 46/125
C. Celata, 47/112
W.W. Chupp, 47/112
S. Chattopadhyay, 47/112
T. Elioff, 90/4040
A. Faltens, 47/112
T. Fessenden, 47/112
A. Garren, 90/4040
D. Gough, 47/112
R. Gough, 50/149
E. Hartwig, 47/112
H. Heckman, 50/245
T. Henderson, 46/161
E. Hoyer, 46/187
R. Johnson, 50A/4119
D. Judd, 47/112
D. Keefe, 47/112
C. Kim, 47/112
M. Krebs, 50A/4112
W. Kunkel, 4/230
G. Lambertson, 47/112
L.J. Laslett, 47/112
E.P. Lee, 47/112
E. Lofgren, 47/112
J. Marx, 46/161
J. Meneghetti, 46/161
H. Meuth, 47/112
J. Peterson, 47/112
C. Pike, 47/112
G. Rosenblatt, 50A/4119
H. Rutkowski, 47/112
A. Sessler, 4/230
D. Shirley, 50A/4133
L. Smith, 47/112
C. Tayler, 46/161
D. Vanecek, 58/101
D. Vaughan, 50/149
A. Warwick, 47/112

Lawrence Livermore Laboratory

Roger Bangerter, L-477
W. Barletta, L-626
Richard J. Briggs, L-321
John L. Emmett, L-488
Dennis Hewitt, L-472
Darwin Ho, L-477
John Holzrichter, L-481
William Kruer, L-472
William Krupke, L-488
Bruce Langdon, L-472
J. Lindl, L-477
Jim Mark, L-477
John Nuckolls, L-477
Louis Reginato, L-526
Erik Storm, L-481

Lockheed

John Siambis

Los Alamos National Laboratory

Ihor Bohachevsky
Richard Cooper
Robert Jameson
Tom McDonald
Earl Meyer
Roger B. Perkins
Richard Stokes
Tai-Sen Wang
Doug Wilson

University of Maryland

Martin Reiser
Derek Tidman

Max Planck Inst. fur
Plasma Physik Garching

Arnulf Schluter

Maxwell Laboratories

Library

National Bureau of Standards

S. Penner
M. Wilson

Naval Research Laboratory

Steven Bodner
T. Coffey
Terry Godlove
Irving Haber
Philip Sprangle
Peter Turchi

Osaka University

T. Mochizuiki
C. Yamanaka

University of Padova

A. Pascolini
M. Pusterla

Physical Dynamics

G.H. Gillespie

Physics International

Library

Pulse Sciences, Inc.

Ian Smith
Kurt Nielson
Mike Tiefenback

RAFAEL

Joseph Shiloh

Rutherford Laboratory

John D. Lawson
Chris Pryor
Graham Rees

Sandia Laboratories

Everet H. Beckner
Don Cook
Glenn Kuswa
Tom Martin
J.P. VanDevender

W.J. Schafer Associates

Michael J. Monsler

SLAC

W. Herrmannsfeldt, Bin 26
B. Richter, Bin 7

Soka University

Tetsuya Saito

SOREQ Nuclear Research Center

A. Sternlieb

TITAN Systems, Inc.

K. Billman
G. Yonas

TRW

J. Gordon
Z. Guiragossian
J. Maniscalco
A.W. Maschke
W. Steele

UCLA

John Dawson

University of Texas at Austin

Toshi Tajima

URA

Edward Knapp

Varian

S.S. Rosenblum

Westinghouse

M. Nahemow
E. W. Sucov

University of Wisconsin

G. Kulcinski
G. Moses
R. Peterson

Other

J.E. Leiss

LAWRENCE BERKELEY LABORATORY
TECHNICAL INFORMATION DEPARTMENT
UNIVERSITY OF CALIFORNIA
BERKELEY, CALIFORNIA 94720